



Enhanced performance through trap states passivation in quantum dot light emitting diode

Mingrui Zhang^a, Feng Guo^a, Qingzhong Zhou^a, Tian Zhong^a, Biao Xiao^{a,b,*}, Liyong Zou^a, Qingliang You^a, Baogui You^c, Yang Li^{c,**}, Xueqing Liu^a, Hongjiao Liu^a, Jun Yan^{d,***}, Jiyan Liu, liujiyan918@163.com^{a,b,****}

^a Key Laboratory of Optoelectronic Chemical Materials and Devices, Ministry of Education, School of Chemical and Environmental Engineering, Jianghan University, Wuhan, 430056, Hubei, China

^b Flexible Display Materials and Technology Co-Innovation Centre of Hubei Province, Jianghan University, Wuhan, 430056, Hubei, China

^c Poly OptoElectronics Tech. Ltd, Jiangmen, 529020, Guangdong, China

^d Department of Physics and Centre for Plastic Electronics, Imperial College London, SW7 2AZ, London, United Kingdom

ARTICLE INFO

Keywords:

Quantum dot light-emitting diodes
Pool-frenkel effect
Trap states

ABSTRACT

Device performance enhancement in quantum dot light-emitting diodes (QLEDs) is realized by adding a small amount of insulating polymer polymethyl methacrylate (PMMA) into the emitting quantum dot layer. Pool-Frenkel effect is observed through temperature-dependent current density-voltage experiments, indicating the important role of trap states, and the addition of the insulating PMMA helps to reduce the Poole-Frenkel barrier hence the trap depth. Reduced density and depth of trap states with PMMA are indeed observed through further capacitance measurements. This work contributes to a better understanding on the effects of traps in QLEDs.

1. Introduction

Colloidal quantum dot-based light-emitting diodes (QLEDs) have attracted considerable interest due to their attractive optical and electronic properties combined with low cost and good solution processability [1–3]. During the past years, extensive studies on new quantum dot materials and device structures have been carried out, and excellent light-emitting performances of QLEDs have been demonstrated [4–6]. In general, efficient charge injection, balanced charge transport, and suppressed nonradiative charge recombination in the quantum dot layer are crucial design criteria for a high-efficiency QLED [7]. Following these principles, minimizing the effects of trap states is usually the top priority since those in-gap traps are detrimental throughout the process of electron-to-photon conversion [8]. The origin of trap states in QDs has been correlated to the vacancies and dangling bonds which are created in the surface modification procedure [9]. In addition, the long organic

ligands in the QD solid film may act as barriers for charge transfer and transport between neighboring QDs [10]. Therefore, great efforts have been taken on tailored passivation schemes based on organic, inorganic, or hybrid scenarios at the atomic scale [11–13]. However, these approaches are usually achieved by chemical synthesis and have the shortcomings of complex and time-consuming operations. A more practical way of suppressing trap states is to simply quantum dots with polymers, such as poly(9-vinylcarbazole) (PVK) [14], poly (para-methyl triphenylamine-*b*-cysteamine acrylamide) [15]. The explanations for the improvement have often been related to the balance of charge transport measured by conventional space-charge-limited-current (SCLC) [16], which is however problematic for disordered materials-based semiconductor devices, therefore may not provide the correct understanding. Therefore, there is still much to be studied to understand what role the trap state plays in this strategy.

In this study, we succeed in enhancing the device performance of

* Corresponding authors. Key Laboratory of Optoelectronic Chemical Materials and Devices, Ministry of Education, School of Chemical and Environmental Engineering, Jianghan University, Wuhan, 430056, Hubei, China.

** Corresponding author.

*** Corresponding authors.

**** Corresponding author. Key Laboratory of Optoelectronic Chemical Materials and Devices, Ministry of Education, School of Chemical and Environmental Engineering, Jianghan University, Wuhan, 430056, Hubei, China.

E-mail addresses: biaoxiao@jhun.edu.cn (B. Xiao), jack.li@polyoe.com (Y. Li), j.yan17@imperial.ac.uk (J. Yan).

QLEDs by adding an insulating polymer polymethyl methacrylate (PMMA) into the emitting quantum dot layer, and perform detailed analysis on the effects of trap states. The charge transport in the QLEDs was analyzed using temperature-dependent current density-voltage measurements. From the analysis, we proved that the Poole-Frenkel (PF) emission was the conduction mechanism in a wide electric field range, and lowered barrier of PF conduction is the reason for improved performance of the PMMA-contained device. Moreover, we recorded capacitance spectra (including C-f and C-V spectra) to confirm the existence and quantify the density of trap states and their distributions. The enhanced performance is ascribed to the passivation of the trap states.

1.1. Experimental methods

Materials: CdO (99%), ZnO (99.9%), Mg(OAc)₂·4H₂O (99%), Zn(OAc)₂·2H₂O (99%), S (99.99%), KOH (98%), DDT (98%), were purchased from Aladdin. Se (99.999%), OA (90%), ODE (90%) were purchased from Alfa Aesar. TBP (99%), was purchased from Shanghai Changgen Chemical technology Co.,Ltd. Ethanol (AR), toluene (AR), n-octane (AR), ethyl acetate (AR) were from Guangdong Guanghua Sci-Tech Co., Ltd. Dimethyl sulfoxide was from Tianjin Baishi Chemical Co., Ltd. All materials are used as received.

Synthesis of luminescent QDs and ZnMgO nanoparticles: For a typical synthesis of CdZnSe/ZnSe/ZnS red emission quantum dots: 0.1 mmol of CdO, 2.5 mmol of ZnO, 5 mL of OA and 8 mL of ODE were mixed in a 50 mL three-neck bottle flask. The mixture was heated to 160 °C and degassed under vacuum for 1 h, then filled with N₂ gas and further heated to 300 °C to get a clear light-yellowish solution. At this temperature, 0.2 mL 2 M Se precursor (dissolved in TBP) was injected swiftly into the flask. The reaction remains at 300 °C for 40 min. To grow ZnSe and ZnS shell, 0.1 mL 2 M Se precursor and 0.1 mL DDT were added dropwise into the flask successively. Each shelling process last for 30 min at 300 °C. After the reaction, the temperature was naturally cooled down to room temperature. The synthesized quantum dots were finally repeated purified using ethanol and toluene and finally dispersed in n-octane. To synthesize 10 wt% magnesium doped ZnO nanoparticles, 0.5 mmol of Mg(OAc)₂·4H₂O and 4.5 mmol Zn(OAc)₂·2H₂O were added into the mixture of 48 mL of dimethyl sulfoxide and 8 mL of absolute ethanol in a three-neck bottle flask, and then vigorously stirred to get a colorless solution. Then 0.4 M potassium hydroxide solution (dissolved in ethanol) dropwise added to the mixture, and the reaction lasted for 3 h. The as-synthesized nanoparticles were washed by ethanol and ethyl acetate, followed by introduction of a certain amount of ethanolamine to stabilize the nanoparticles. The sample was finally dispersed in absolute ethanol for further use.

Device fabrication. The QLEDs with a structure of ITO/PEDOT:PSS/TFB/PMMA modified QDs (or pure QDs)/ZnMgO/Al were fabricated. Pre-patterned ITO glass substrates were firstly cleaned using consecutive ultrasonic baths in acetone, detergent, deionized water, and isopropyl alcohol, respectively. The substrates were treated with oxygen plasma for 5 min, and then a 40 nm-thick poly(styrene sulfonate)-doped poly(ethylenedioxothiophene) (PEDOT: PSS, Clevios AI 4083) film was obtained by spin-coating on the ITO-coated glass. The substrates were subsequently dried at 150 °C. After that, the hole transport material TFB (purchased from LUMTEC Inc.), dissolved in chlorobenzene with a concentration of 10 mg/mL, was spin-casted at 3000 rpm for 30 s in a N₂-glovebox and baked at 120 °C for 10 min. The QDs were dispersed in octane with a total concentration of 30 mg/mL, and different amounts of PMMA were added to form mixed solutions. Then the solutions were spin-coated at 2000 rpm and baked at 100 °C for 10 min. It is worth noting that the content of PMMA should not be too high, otherwise it will affect the dispersion of the solution, as shown in Figure S1. After that, ZnMgO nanoparticles, dispersed in ethanol with a concentration of 30 mg/mL, were spin-coated as electron transport layer at 3000 rpm and baked at 100 °C for 10 min. To complete the device, a 70 nm thick layer

of Al was thermally evaporated in a vacuum chamber at 1 × 10⁻⁵ Pa.

Device Characterization. The current density-voltage-luminance characteristics were measured using a Keithley 2450 source meter and a Konica Minolta luminance meter LS-150. The electroluminescence spectra were collected using a Topcon SR-UL2 Spectroradiometer. The photoluminescence spectra were obtained using a fluorescence spectrometer (Edinburgh, FLS 920). The capacitance spectra were recorded using an impedance analyzer (Keysight, E4990A). The optical permittivity was measured using a dual rotating-compensator Mueller matrix ellipsometer (Wuhan Optics Technology Co., ME-L ellipsometer). The low temperature environment in the experiments was provided by a cryostat system (Janis, ST-100).

2. Results and discussion

The multilayer structure of the QLEDs studied, herein, is ITO/PEDOT:PSS/poly[(9,9-diptylfluorenyl-2,7-diyl)-*alt*-(4,40-(N-(4-butyl-phenyl)))](TFB)/PMMA modified QDs (or pure QDs)/Mg doped ZnO (ZnMgO)/Al, as presented in Fig. 1a. In this device configuration, ITO, PEDOT:PSS, TFB, QDs, ZnMgO and Al were chosen as anode, hole injection layer, hole transport layer, light emitting layer, electron transport layer and cathode, respectively. To demonstrate the efficacy of PMMA, devices with emitting layers of pure QDs and PMMA modified QDs were fabricated under identical processing conditions. The electroluminescence spectra (EL) of the devices are shown in Fig. 1b. All devices exhibited saturated red emission with a central emission wavelength of 618 nm and a full width at half maximum (FWHM) of about 23 nm, indicating that PMMA did not change the color coordinates.

Fig. 1c depicts typical current density-voltage-luminance (*J-V-L*) results of the devices. The QLED with 2% PMMA shows the highest current density, followed by the device containing 1% PMMA, while the device without PMMA presents the worst voltage response. The turn-on voltage (*V_{on}*) decreased from 2.58 V to 2.02 V when 1% PMMA was added into the QD layer, and the maximum brightness was enhanced from 27,621 cd/m² to 164,690 cd/m². Although the *V_{on}* decreased further to 1.97 V when the content of PMMA reached 2%, increasing the amount of PMMA results in worse device performance since the luminescence maximum greatly reduced to 133,700 cd/m². More intuitive phenomena can be found in the current efficiency *versus* luminance curves, as shown in Fig. 1d. It is seen that the current efficiency is very sensitive to the amount of PMMA. By adding PMMA into the QD layer, the performance of the device is improved. It reaches the highest efficiency in the 1% PMMA-added QLEDs with a maximum current efficiency of 26.28 cd/A, which is 2.2-fold higher than that of the control device (pure QDs) with a maximum current efficiency of 11.94 cd/A. When the ratio of PMMA is further increased, the QLED device exhibits decreased current efficiency. Similar results can also be found in the green QD-based devices, which are presented in Figure S2 in the Supporting Information.

To obtain insights into the role of PMMA in the device efficiency improvement, a series of characterizations and analysis were carried out. Early studies generally believed that mixing a small number of organic molecules into the QD layer could improve the charge balance in the QLEDs [14–16]. To verify this, charge transport properties in the devices were studied through the conventional space-charge-limited current (SCLC) method as what has been done before [17]. In Figure S3, the effects of the PMMA content on the charge carrier mobilities are presented and compared. In fact, a wide distribution of electron and hole mobilities could be observed in all the devices. For example, the hole and electron mobilities in the 2% PMMA-based device span several orders of magnitude from 10⁻⁸ to 10⁻¹² m² V⁻¹ s⁻¹ and 10⁻⁹ to 10⁻¹² m² V⁻¹ s⁻¹, respectively. Such a wide distribution of mobilities indicates that conventional SCLC-based method is not a reliable approach for QD materials because of the polydisperse nature of the organic charge injection/transport layers or/and the low crystallinity of

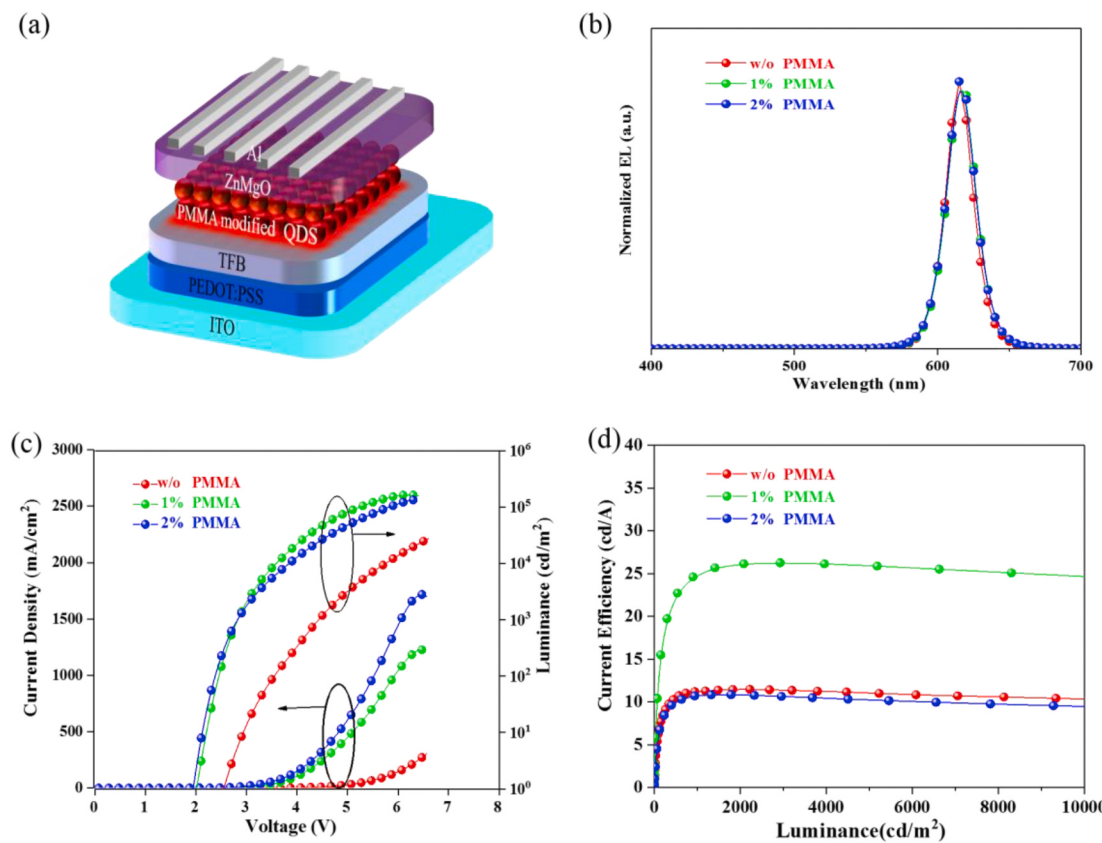


Fig. 1. (a) Schematic of the QLED device configuration. (b) Normalized EL spectra of QLEDs based on different emitting layers. (c) Current density-voltage-luminance and (d) Current efficiency-luminance characteristics.

the inorganic ZnMgO and QD thin films. Since there exist vast numerical overlaps in the mobility values, it is difficult to draw a conclusion whether adding PMMA into the QD layer could alleviate the charge imbalance in the devices using SCLC. Also, we note here that quantitative analysis of charge transport with traps for disordered materials is very difficult, and the method and extracted value varies in the literature. Instead, our approach is to study the charge transport behavior from the perspective of trap states (trap density and its distribution), which should provide much better insight than SCLC mobilities alone.

Since the traps are closely related to the charge transport mechanism in semiconductor devices [18,19], we first employ temperature-dependent current density-voltage measurements to explore the effect of traps on the charge conduction behaviors in the QLEDs. Fig. 2a, 2c and 2e show the current density-voltage curves of the devices measured in the temperature range of 150 K–270 K. To facilitate analysis, data are presented in a $\ln(I/V)$ vs $1/V^{1/2}$ form. It is seen that the current density in the device is temperature-dependent, and its value increases at a higher temperature. In addition, there are very good linear correlations between $\ln(I/V)$ and $1/V^{1/2}$. Good linearity can also be found between $\ln(I)$ and $1/T$. For instance, we randomly extract a set of current values and plot them against $1/T$, the correlation coefficients (R^2) of the linear fits are very close to 1, as shown in Fig. 2b, d and 2f. Based on the correlation between current density and voltage and the dependence of current density on the temperature, we believe that the Poole-Frenkel emission is the charge transport mechanism in QLEDs, therefore trap states play an important role [20,21].

Fig. 3 illustrates the Poole-Frenkel emission process in the quantum dot layer. Essentially, the Poole-Frenkel effect describes the increase of the thermal emission rate of carriers in an external electric field due to the reduction of the barrier. Take the electron emission as an example, in the absence of an electric field, the minimum energy for an electron to escape from a trap state is $q\Phi_{t,n}$ (where q is the elementary charge). This

value decreases by $q\Delta\Phi_{PF,n}$ when a forward electric field is applied, where the barrier reduction $q\Delta\Phi_{PF,n}$ is given by [22].

$$q\Delta\Phi_{PF,n} = [(q^3E)/(\pi\varepsilon_0\varepsilon_{r,opt})]^{1/2}, \quad (1)$$

Here, E is the electric field intensity, ε_0 the vacuum permittivity, and $\varepsilon_{r,opt}$ the relative optical permittivity of the QD layer. The estimated values of $\varepsilon_{r,opt}$ using ellipsometry in the PMMA-contained QD layers are lower than that in the pristine QD layer (as shown in Fig. 3b), which means that the trapped charges in the PMMA-contained QLEDs are possibly easier to be activated and the currents in these devices should be higher, consistent with the current density-voltage curves in Fig. 1c.

Capacitance-voltage (C-V) measurements were carried out at different temperatures to further study the trap states in the devices, as shown in Fig. 4a–c. For all the devices within the temperature range of measurements, the capacitance values are almost constant at low voltages, indicating that the devices are completely depleted. With increased applied voltages, the internal field drops, and we see a spike when the applied voltage approaches the built-in potential, and the height of the spike increases with temperature. These observations can be rationalized by the dynamics involving trap states. First of all, the trapped charges with a release frequency close to probe frequency can be detected [23]. At high temperature, 280 K for example, we see that the capacitance enhancement when the applied voltage is close to the built-in voltage is present in all devices with or without PMMA, suggesting the existence of trap state in all devices at that temperature. In addition, devices with PMMA show much higher capacitance enhancement than PMMA-free device suggesting that those trap states are high in energy, therefore presenting a shallower trap depth and easy to probe in the PMMA devices. Secondly, with reduced temperature, we see a fast drop of this height because only lower energy states are filled and cannot be detected by the same frequency used for high temperature. These observations are strong evidence of trap states mediated charge

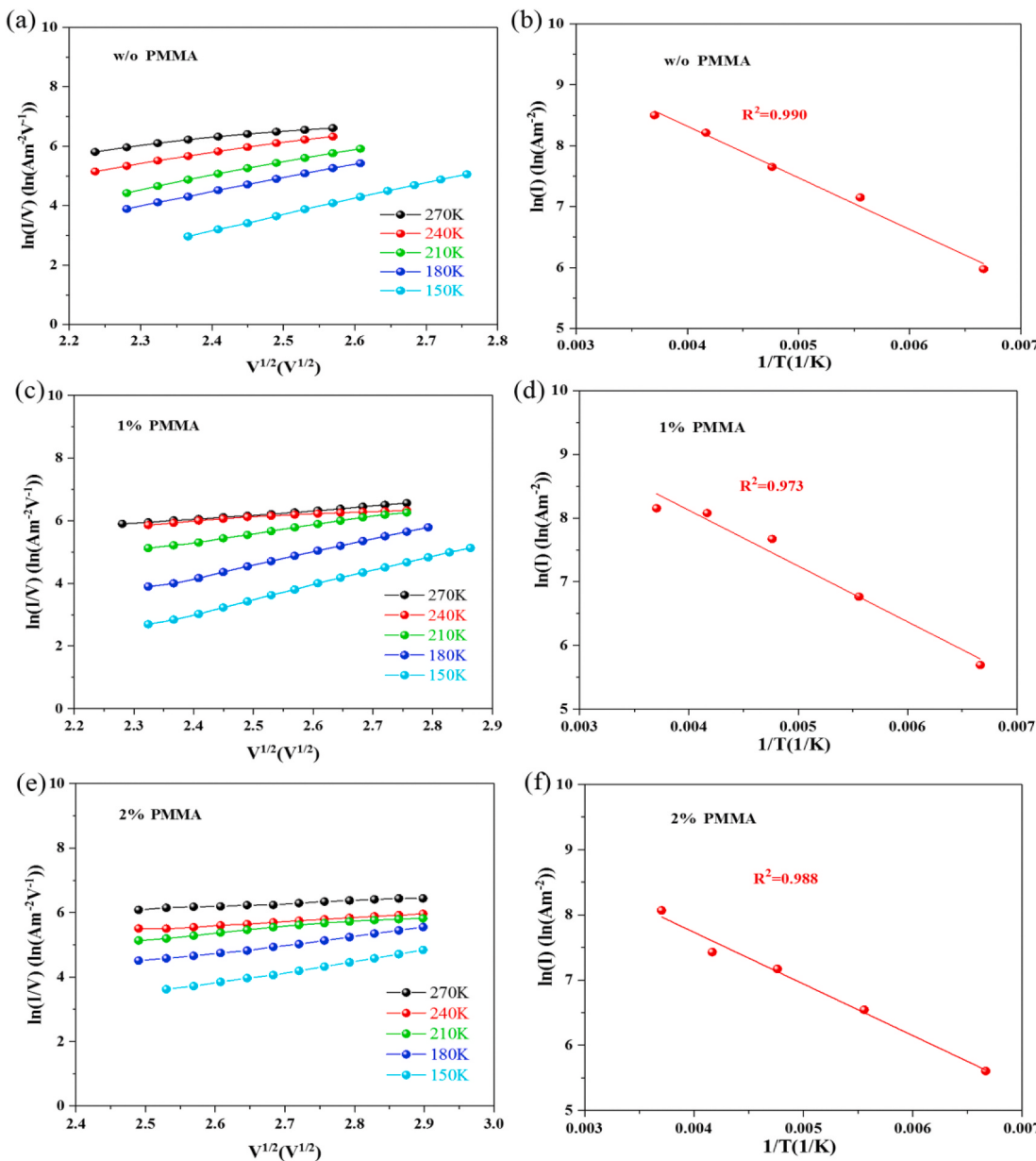


Fig. 2. Typical current density-voltage curves plotted in a $\ln(I/V)$ vs $1/V^{1/2}$ form for QLEDs (a) without, (c) with 1% and (e) with 2% PMMA at different temperatures. (b), (d) and (f) are the dependence of device current densities extracted at 6.6 V on temperature. The straight lines are linear fits to the experimental data.

dynamics in QLEDs, and devices with PMMA possibly have a narrower distribution of trap states than PMMA-free device.

To confirm the observation above, we further quantify the density and distribution of trap states using capacitance-frequency characteristics, as shown in Fig. 5a. For all the devices, the curves exhibit an increasing trend as the frequency decreases, which again indicates the existence of the trap states located in the band gap [24]. The distribution of trap states therefore can be estimated [24,25]. Fig. 5b presents the estimated trap distributions at room temperature. The experimental data is analyzed using Gaussian distribution function. It is seen that the QLED without PMMA shows the broadest trap distribution and a total concentration of $1.50 \times 10^{17} \text{ cm}^{-3}$. In contrast, the adding of 1% PMMA into the QD layer shows a narrowed trap distribution, which agree with the conclusion drawn using C-V analysis. In addition, we also observe reduced density of traps to $5.74 \times 10^{16} \text{ cm}^{-3}$. Therefore, the addition of PMMA could reduce the trap depth as well as the density, indicating that the trap states in the QLED can be largely passivated with the addition of a small amount of PMMA. The addition of 2% PMMA shows narrower

trap states distribution than PMMA free device again agreeing with C-V analysis, however the trap concentration grows to $1.49 \times 10^{17} \text{ cm}^{-3}$. This phenomenon can be understood because large amount of insulating polymer will form additional traps in the QD layer [10], preventing electrons from traveling between the quantum dots.

It is known that the trap states are detrimental to the emission property of QLEDs because of the additional non-radiative relaxation [26]. In order to study the effects of PMMA on passivation of non-radiative channels, photoluminescence (PL) measurements were performed, and the results are shown in Fig. 6a. The PL intensity of the QDs becomes substantially higher when 1% PMMA is added, and this behavior is caused by the decreased non-radiative recombination. While a lower PL intensity is observed in the device with 2% PMMA. The transient fluorescence spectra of the QD films are shown in Fig. 6b. The fluorescence lifetime of the quantum dot film containing 1% PMMA is 20.1 ns, while the lifetime of the quantum dot film without PMMA and containing 2% PMMA is 13.6 ns and 14.4 ns, respectively. Obviously, appropriate content of PMMA is conducive for the extension of the

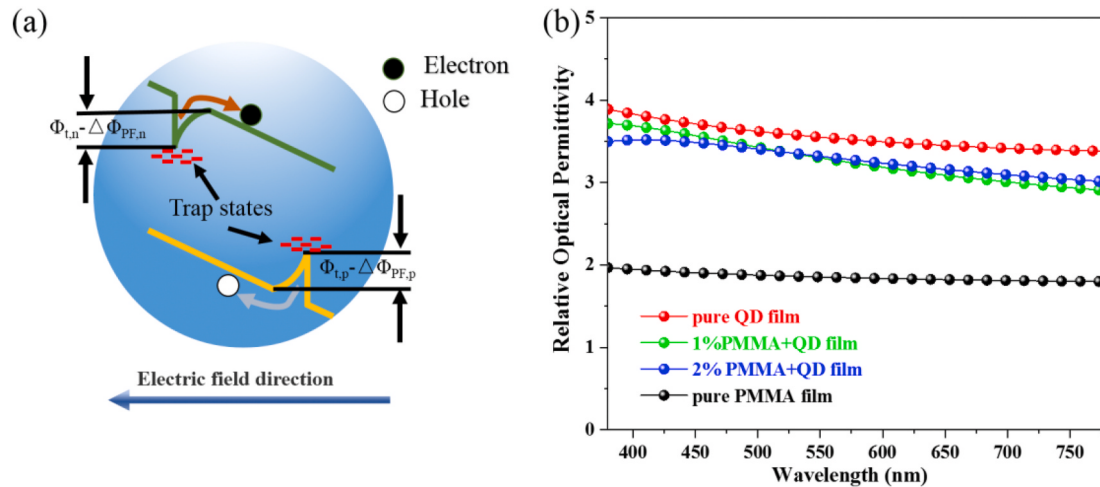


Fig. 3. (a) Illustration of the charge conduction mechanism in the QLEDs. $\Phi_{t,n}$ and $\Phi_{t,p}$ are trap levels for electrons and holes; $\Delta\Phi_{PF,n}$, $\Delta\Phi_{PF,p}$ are barriers reduction for electrons and holes, respectively. (b) Relative optical permittivity of the QD layers with different PMMA contents.

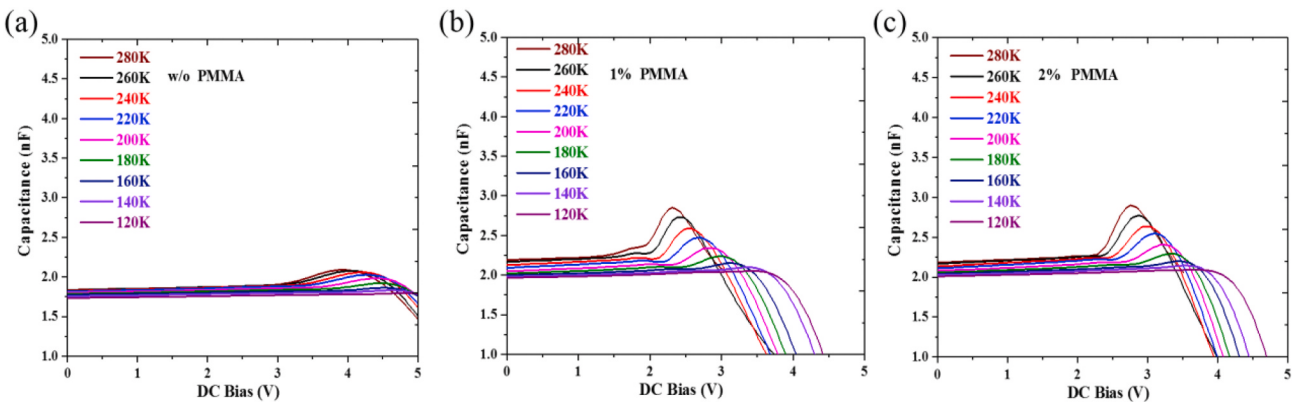


Fig. 4. Capacitance-voltage curves of device (a) without, (b) 1% and (c) 2% PMMA. These measurements were performed at a low frequency of 10 kHz, and the amplitude of the AC signal is 50 mV.

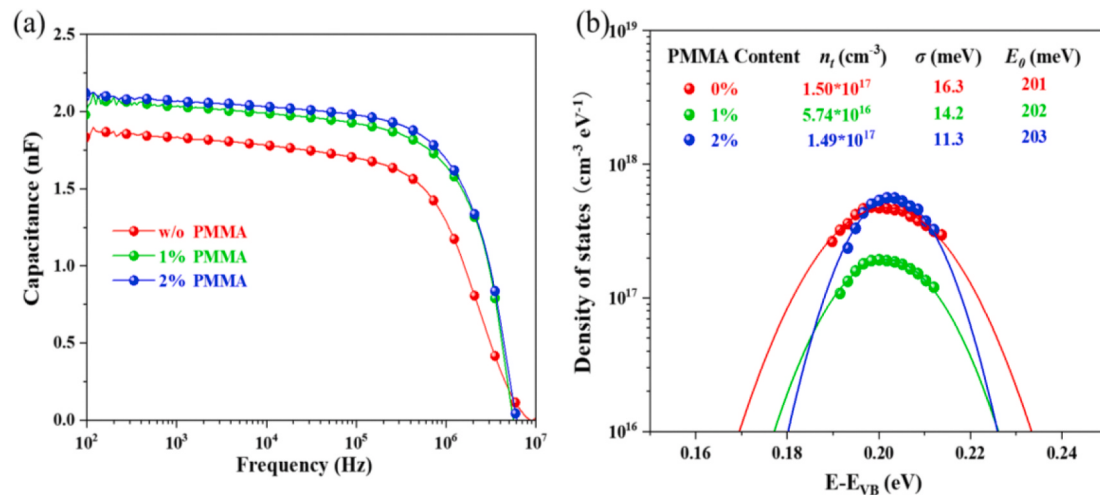


Fig. 5. (a) Capacitance spectra of QLEDs with various PMMA contents measured at zero bias voltage. (b) Trap density distribution with respect to the QD conduction band. The solid lines are fitting results from Gaussian distribution function $g_c(E) = \frac{n_t}{\sqrt{2\pi}\sigma} \exp\left[-\frac{(E_0-E)^2}{2\sigma^2}\right]$, where n_t is the total trap density, σ the width of the Gaussian type of trap distribution and E_0 the average energy.

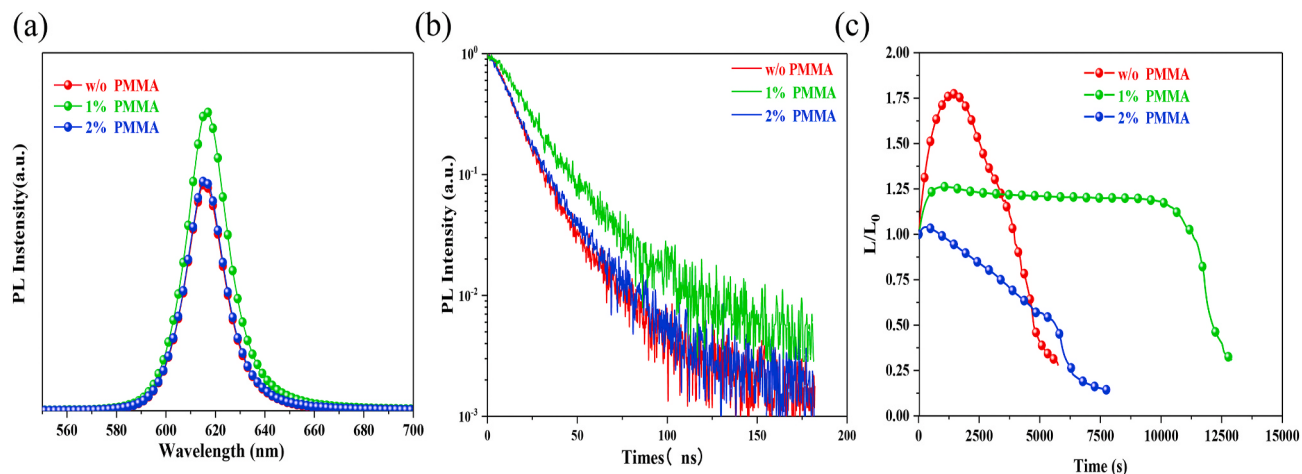


Fig. 6. (a) Photoluminescence spectra (b) Transient PL spectra of the QD films with different PMMA contents and (c) Degradation of QLEDs with different PMMA contents.

fluorescence lifetime of quantum dots. In addition, photoluminescence quantum yields are measured to be 62%, 73% and 42% for the QD film with 0, 1% and 2% PMMA, respectively, suggesting that additional recombination channels are created by the excessive PMMA. Fig. 6c shows the results of stability measurements. The initial luminance (L_0) is fixed at 10,000 cd/m², and the devices were tested in air at room temperature without encapsulation. In the beginning period, the curves showed an upward trend. This positive aging effect could be explained by the interfacial reaction between Al and ZnMgO [27]. The LT80 lifetimes (luminance reduction to 80% of the original value) for the devices with 0, 1% and 2% PMMA are 4328 s, 11,742 s and 2940 s, respectively. In other words, device with the lowest trap concentration has the most stable luminous performance. This result is in line with expectations because traps lead to non-radiative recombination centers for excitons, which also results in a decrease in luminance [28–30].

3. Conclusions

In summary, we demonstrated enhanced device performance in QLEDs by adding a small amount of insulating polymer PMMA to the emitting layer. The device with 1% polymer additive shows a current efficiency of 26.28 cd/A, which is 2.2-fold of that in the pristine device. Meanwhile, the turn-on voltage in the PMMA-contained device reduced greatly. The charge transport mechanism in the QLEDs was investigated by a temperature-variable current density-voltage technique. It was found that the charge transport follows the Poole-Frenkel emission mechanism in QLEDs and the addition of low dielectric constant material into the QD layer facilitates charge conduction. Capacitance spectra (including C-f and C-V spectra) were recorded to confirm the existence of trap states and their distributions. The enhanced performance is ascribed to the passivation of the trap states. These results suggest that the trap-passivation strategy is simple but highly promising toward high-efficiency QLEDs.

Author contribution statement

B. X. and M. Z. conceived the idea and designed the experiments. M. Z. fabricated the devices. F. G., Q. Z., T. Z. L. Z. and Q. Y. conducted electrical characterizations. B. Y. and Y. L. synthesized the quantum dots. X. L. H. L. J. Y. and J. L. conducted optical tests. All authors contributed to manuscript preparation, data analysis and interpretation, and discussed the results.

Declaration of competing interest

The authors declare that they have no known competing financial interests or personal relationships that could have appeared to influence the work reported in this paper.

Acknowledgment

The authors thank the Natural Science Foundation of Hubei Province (No. 2019CFB198), the Guiding Project of Education Department of Hubei Province (No. B2018259), the Central Leading Local Scientific Research Project (No. 2019ZYYD005), and Key-Area Research and Development Program of Guangdong Province (NO. 2019B010924001) for the financial support. We acknowledge the help of Jiangmen Innovative & Entrepreneurial Research Team Program in synthesizing quantum dots.

Appendix A. Supplementary data

Supplementary data to this article can be found online at <https://doi.org/10.1016/j.jlumin.2021.117946>.

References

- [1] J.M. Pietryga, Y.-S. Park, J. Lim, A.F. Fidler, W.K. Bae, S. Brovelli, V.I. Klimov, Spectroscopic and device aspects of nanocrystal quantum dots, *Chem. Rev.* 116 (2016) 10513.
- [2] X. Dai, Y. Deng, X. Peng, Y. Jin, Quantum-dot light-emitting diodes for large-area displays: towards the dawn of commercialization, *Adv. Mater.* 29 (2017) 1607022.
- [3] H. Moon, C. Lee, W. Lee, J. Kim, H. Chae, Stability of quantum dots, quantum dot films, and quantum dot light-emitting diodes for display applications, *Adv. Mater.* (2019) 1804294.
- [4] Y.-H. Won, O. Cho, T. Kim, D.-Y. Chung, T. Kim, H. Chung, H. Jang, J. Lee, D. Kim, E. Jang, Highly efficient and stable InP/ZnSe/ZnS quantum dot light-emitting diodes, *Nature* 575 (2019) 634.
- [5] H. Shen, Q. Gao, Y. Zhang, Y. Lin, Q. Lin, Z. Li, L. Chen, Z. Zeng, X. Li, Y. Jia, S. Wang, Z. Du, L.S. Li, Z. Zhang, Visible quantum dot light-emitting diodes with simultaneous high brightness and efficiency, *Nat. Photon.* 13 (2019) 192.
- [6] X. Dai, Z. Zhang, Y. Jin, Y. Niu, H. Cao, X. Liang, L. Chen, J. Wang, X. Peng, High-performance light-emitting diodes based on quantum dots, *Nature* 515 (2014) 96.
- [7] J. Lim, W.K. Bae, J. Kwak, S. Lee, C. Lee, K. Char, Perspective on synthesis, device structures, and printing processes for quantum dot displays, *Opt. Mater. Express* 2 (2012) 594.
- [8] C. Giansant, I. Infante, Surface traps in colloidal quantum dots: a combined experimental and theoretical perspective, *J. Phys. Chem. Lett.* 8 (2017) 5209.
- [9] R. Wang, Y. Shang, P. Kanjanaboons, W. Zhou, Z. Ning, E.H. Sargent, Colloidal quantum dot ligand engineering for high performance solar cells, *Energy Environ. Sci.* 9 (2016) 1130.
- [10] P.R. Brown, D. Kim, R.R. Lunt, N. Zhao, M.G. Bawendi, J.C. Grossman, V. Bulović, Energy level modification in lead sulfide quantum dot thin films through ligand exchange, *ACS Nano* 8 (2014) 5863.

- [11] J. Tang, K.W. Kemp, S. Hoogland, K.S. Jeong, H. Liu, L. Levina, M. Furukawa, X. Wang, R. Debnath, D. Cha, K.W. Chou, A. Fischer, A. Amassian, J.B. Asbury, E.H. Sargent, Colloidal-quantum-dot photovoltaics using atomic-ligand passivation, *Nat. Mater.* 10 (2011) 765.
- [12] Z. Ning, Y. Ren, S. Hoogland, O. Voznyy, L. Levina, P. Stadler, X. Lan, D. Zhitomirsky, E.H. Sargent, All-inorganic colloidal quantum dot photovoltaics employing solution-phase halide passivation, *Adv. Mater.* 24 (2012) 6295.
- [13] A.H. Ip, S.M. Thon, S. Hoogland, O. Voznyy, D. Zhitomirsky, R. Debnath, L. Levina, L.R. Rollny, G.H. Carey, A. Fischer, K.W. Kemp, I.J. Kramer, Z. Ning, A.J. Labelle, K.W. Chou, A. Amassian, E.H. Sargent, Hybrid passivated colloidal quantum dot solids, *Nat. Nanotechnol.* 7 (2012) 577.
- [14] F. Liang, Y. Liu, Y. Hu, Y.-L. Shi, Y.-Q. Liu, Z.-K. Wang, X.-D. Wang, B.-Q. Sun, L.-S. Liao, Polymer as an additive in the emitting layer for high-performance quantum dot light-emitting diodes, *ACS Appl. Mater. Interfaces* 9 (2017) 20239.
- [15] M. Zorn, W.K. Bae, J. Kwak, H. Lee, C. Lee, R. Zentel, K. Char, Quantum dot-block copolymer hybrids with improved properties and their application to quantum dot light-emitting devices, *ACS Nano* 3 (2009) 1063.
- [16] L. Chen, S. Wang, K. Zhang, A. Wang, Y. Fang, Z. Du, Enhanced performances of quantum dot light-emitting diodes with PFN-adding emitting layer, *Org. Electron.* 66 (2019) 110.
- [17] A. Rose, Space-charge-limited currents in solids, *Phys. Rev.* 97 (1955) 1538.
- [18] A.J. Campbell, D.D.C. Bradley, D.G. Lidzey, Space-charge limited conduction with traps in poly (phenylene vinylene) light emitting diodes, *J. Appl. Phys.* 82 (1997) 6326.
- [19] S. Yu, X. Guan, H.-S.P. Wong, Conduction mechanism of TiN/HfO_x/Pt resistive switching memory: a trap-assisted-tunneling model, *Appl. Phys. Lett.* 99 (2011), 063507.
- [20] J.-C. Li, D. Wang, D.-C. Ba, Effects of temperature and light illumination on the current-voltage characteristics of molecular self-assembled monolayer junctions, *J. Phys. Chem. C* 116 (2012) 10986.
- [21] S.D. Ganichev, E. Ziemann, W. Prettl, J.N. Yassievich, A.A. Istratov, E.R. Weber, Distinction between the poole-frenkel and tunneling models of electric-field-stimulated carrier emission from deep levels in semiconductors, *Phys. Rev. B* 61 (2000) 10361.
- [22] J.G. Simmons, Poole-frenkel effect and Schottky effect in metal-insulator-metal systems, *Phys. Rev.* 155 (1967) 657.
- [23] D. Ray, L. Burfone, K. Leo, M. Riede, Detection of trap charge in small molecular organic bulk heterojunction solar cells, *Phys. Rev. B* 82 (2010) 125204.
- [24] D. Bozyigit, S. Volk, O. Yarema, V. Wood, Quantification of deep traps in nanocrystal solids, their electronic properties, and their influence on device behavior, *Nano Lett.* 13 (2013) 5284.
- [25] T. Walter, R. Herberholz, C. Muller, H.W.J. Schock, Determination of defect distributions from admittance measurements and application to Cu(in,Ga)Se₂ based heterojunctions, *Appl. Phys.* 80 (1996) 4411.
- [26] W.K. Bae, Y.-S. Park, J. Lim, D. Lee, L.A. Padilha, H. McDaniel, I. Robel, C. Lee, J. M. Pietryga, V.I. Klimov, Controlling the influence of auger recombination on the performance of quantum-dot light-emitting diodes, *Nat. Commun.* 4 (2013) 2661.
- [27] Q. Su, Y. Sun, H. Zhang, S. Chen, Origin of positive aging in quantum-dot light-emitting diodes, *Adv. Sci.* 5 (2018) 1800549.
- [28] H. Aziz, Z.D. Popovic, Degradation phenomena in small-molecule organic light-emitting devices, *Chem. Mater.* 16 (2004) 4522.
- [29] F. So, D. Kondakov, Degradation mechanisms in small-molecule and polymer organic light-emitting diodes, *Adv. Mater.* 22 (2010) 3762.
- [30] S. Schmidbauer, A. Hohenleutner, B. König, Chemical degradation in organic light-emitting devices: mechanisms and implications for the design of new materials, *Adv. Mater.* 25 (2013) 2114.

Supporting Information

Enhanced performance through trap states passivation in quantum dot light emitting diode

*Mingrui Zhang^a, Feng Guo^a, Qingzhong Zhou^a, Tian Zhong^a, Biao Xiao^{*a,b}, Liyong Zou^a,
Qingliang You^a, Baogui You^c, Yang Li^{*c}, Xueqing Liu^a, Hongjiao Liu^a, Jun Yan^{*d}, Jiyan Liu^{*a,b}*

^a Key Laboratory of Optoelectronic Chemical Materials and Devices, Ministry of Education,
School of Chemical and Environmental Engineering, Jianghan University, Wuhan 430056, Hubei,
China

^b Flexible Display Materials and Technology Co-Innovation Centre of Hubei Province, Jianghan
University, Wuhan 430056, Hubei, China

^c Poly OptoElectronics Tech. Ltd, Jiangmen 529020, Guangdong, China

^d Department of Physics and Centre for Plastic Electronics, Imperial College London, SW7 2AZ,
London, United Kingdom

Experimental Methods

Materials: CdO (99%), ZnO (99.9%), Mg(OAc)₂·4H₂O (99%), Zn(OAc)₂·2H₂O (99%), S (99.99%), KOH (98%), DDT (98%), were purchased from Aladdin. Se (99.999%), OA (90%), ODE (90%) were purchased from Alfa Aesar. TBP (99%), was purchased from Shanghai Changgen Chemical technology Co.,Ltd. Ethanol (AR), toluene (AR), n-octane (AR), ethyl acetate (AR) were from Guangdong Guanghua Sci-Tech Co., Ltd. Dimethyl sulfoxide was from Tianjin Baishi Chemical Co., Ltd. All materials are used as received.

Synthesis of luminescent QDs and ZnMgO nanoparticles: For a typical synthesis of CdZnSe/ZnSe/ZnS red emission quantum dots: 0.1 mmol of CdO, 2.5 mmol of ZnO, 5 mL of OA and 8 mL of ODE were mixed in a 50 mL three-neck bottle flask. The mixture was heated to 160°C and degassed under vacuum for 1 hour, then filled with N₂ gas and further heated to 300°C to get a clear light-yellowish solution. At this temperature, 0.2mL 2M Se precursor (dissolved in TBP) was injected swiftly into the flask. The reaction remain at 300°C for 40 min. To grow ZnSe and ZnS shell, 0.1mL 2M Se precursor and 0.1mL DDT were added dropwise into the flask successively. Each shelling process last for 30 min at 300°C. After the reaction, the temperature was naturally cooled down to room temperature. The synthesized quantum dots were finally repeated purified using ethanol and toluene and finally dispersed in n-octane. To synthesize 10 wt% magnesium doped ZnO nanoparticles, 0.5 mmol of Mg(OAc)₂·4H₂O and 4.5 mmol Zn(OAc)₂·2H₂O were added into the mixture of 48mL of dimethyl sulfoxide and 8 mL of absolute ethanol in a three-neck bottle flask, and then vigorously stirred to get a colorless solution. Then 0.4M potassium hydroxide solution (dissolved in ethanol) dropwise added to the mixture, and the reaction lasted for three hours. The as-synthesized nanoparticles were washed by ethanol and ethyl

acetate, followed by introduction of a certain amount of ethanolamine to stabilize the nanoparticles. The sample was finally dispersed in absolute ethanol for further use.

Device fabrication. The QLEDs with a structure of ITO / PEDOT:PSS / TFB / PMMA modified QDs (or pure QDs) / ZnMgO / Al were fabricated. Pre-patterned ITO glass substrates were firstly cleaned using consecutive ultrasonic baths in acetone, detergent, deionized water, and isopropyl alcohol, respectively. The substrates were treated with oxygen plasma for 5 min, and then a 40 nm-thick poly(styrene sulfonate)-doped poly(ethylenedioxythiophene) (PEDOT: PSS, Clevios AI 4083) film was obtained by spin-coating on the ITO-coated glass. The substrates were subsequently dried at 150 °C. After that, the hole transport material TFB (purchased from LUMTEC Inc.), dissolved in chlorobenzene with a concentration of 10 mg/mL, was spin-casted at 3000 rpm for 30 s in a N₂-glovebox and baked at 120 °C for 10 min. The QDs were dispersed in octane with a total concentration of 30 mg/mL, and different amounts of PMMA were added to form mixed solutions. Then the solutions were spin-coated at 2000 rpm and baked at 100 °C for 10 min. It is worth noting that the content of PMMA should not be too high, otherwise it will affect the dispersion of the solution, as shown in Figure S1. After that, ZnMgO nanoparticles, dispersed in ethanol with a concentration of 30 mg/mL, were spin-coated as electron transport layer at 3000 rpm and baked at 100 °C for 10 min. To complete the device, a 70 nm thick layer of Al was thermally evaporated in a vacuum chamber at 1 × 10⁻⁵ Pa.

Device Characterization. The current density-voltage-luminance characteristics were measured using a Keithley 2450 source meter and a Konica Minolta luminance meter LS-150. The electroluminescence spectra were collected using a Topcon SR-UL2 Spectroradiometer. The photoluminescence spectra were obtained using a fluorescence spectrometer (Edinburgh, FLS 920). The capacitance spectra were recorded using an impedance analyzer (Keysight, E4990A).

The optical permittivity was measured using a dual rotating-compensator Mueller matrix ellipsometer (Wuhan Eoptics Technology Co., ME-L ellipsometer). The low temperature environment in the experiments was provided by a cryostat system (Janis, ST-100).

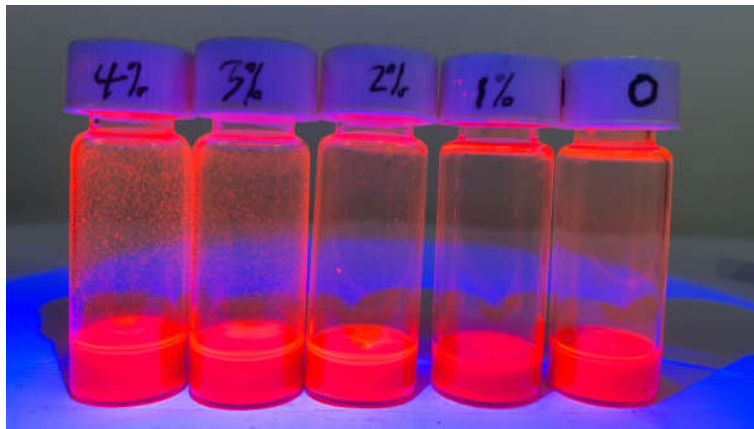


Figure S1. Photoluminescence photos of the PMMA-contained solutions after shaking under UV light.

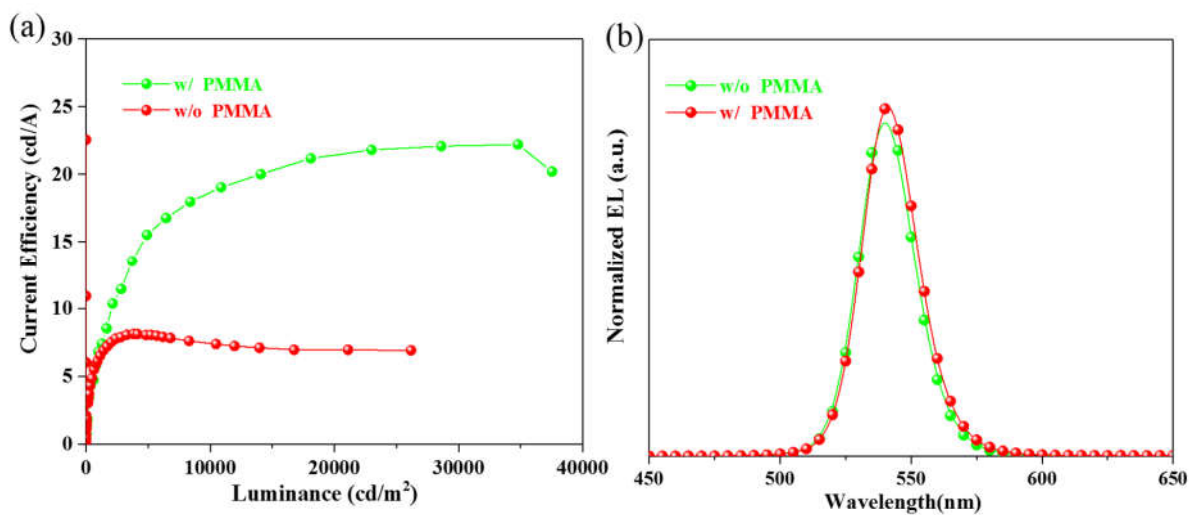


Figure S2. (a) Current efficiency-luminance characteristics and (b) Normalized EL spectra of green QLEDs without PMMA or with 1% PMMA.

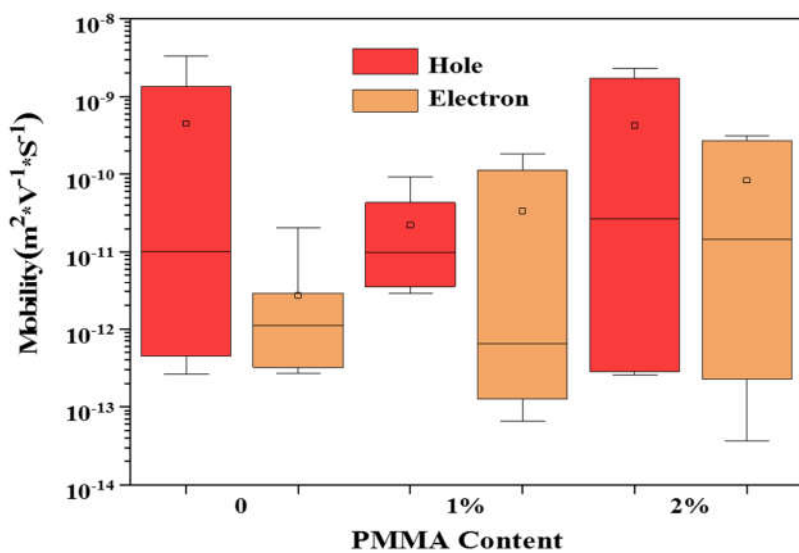


Figure S3. Charge carrier mobilities of the QLEDs with various PMMA content measured by the SCLC method.